JOC The Journal of Organic Chemistry

Article

pubs.acs.org/joc

Synthesis and Thermal Stability of Benzoxazine Nitroxides

Paola Astolfi and Pierluigi Stipa*

S.I.M.A.U. Department - Chemistry Division, Università Politecnica delle Marche, via Brecce Bianche, I-60131 Ancona, Italy

Supporting Information

ABSTRACT: A new class of stable nitroxides (aminoxyls) having a 1,4-benzoxazine structure were synthesized and the corresponding thermal stability tested. All derivatives were stable in the entire range of temperatures employed, except those having a benzyl or a *tert*-butyl group at the β-position with respect to the aminoxyl function, which underwent radical fragmentation. Such a behavior allowed a kinetic study, carried out by means of EPR spectroscopy, to determine the corresponding rate constants and activation parameters (E_a). Appropriate DFT calculations were performed for all nitroxides including also the thermally stable ones, in order to study the geometries of the fragmentation transition States as well as to compute the corresponding bond dissociation enthalpies (BDH), useful for further modeling purposes. The data obtained were interpreted on the basis of the relative stability of the leaving radical, according to the corresponding E_a and BDH, whereas in the case of *tert*-butyl derivatives steric hindrance should play a determinant role, as evidenced by a comparison of the geometric, kinetic, and thermodynamic parameters upon the whole series.

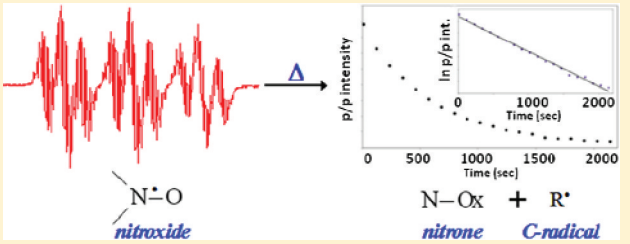

INTRODUCTION

Aminoxyls (nitroxides) represent an interesting class of persistent organic free radicals. In some cases, they are stable and commercially available and have been widely used for years as spin probes,[1] spin labels,[2] contrast agents,[3] spin carriers in molecular magnetic materials,[4] and antioxidants in polymeric[5] as well as in biological systems.[6] The antioxidant activity of these compounds has mainly been attributed to their attitude to give very fast radical−radical coupling reactions with carbon-centered radicals.[7] Their reactivity toward oxygen-centered radicals still remains not well established,[8] except for the case of aromatic aminoxyls in which the delocalization of the free valence in an aromatic π system is possible,[9,10] as with indolinonic nitroxides.[11]

At the same time, electron paramagnetic resonance (EPR) probably represents the simplest and the most useful experimental technique to directly detect and characterize free radicals whose persistency allows the acquisition of their EPR signals: from the full spectral analysis hyperfine coupling constant (hfcc) values useful for building correlations concerning the structure of the detected radical can be obtained. However, in certain cases the correct interpretation of these signals is not straightforward for the presence of a large number of lines, but some improvements in density functional theory (DFT)[12] have recently led to computational methods able to describe the properties of free radicals, including their EPR features, with an excellent level of confidence.[10,13]

For years, our group has been involved in the synthesis and reactivity of indolinonic nitroxides,[11,14] also used as additives in polymers.[15] In particular, these derivatives have been proposed not only as antioxidants but also, once transformed in the corresponding alkoxyamines, as initiators in the controlled nitroxide-mediated polymerization (NMP) of methyl methacrylate.[16] However, considering the relatively high temperatures typical of some industrial processes in which polymers and nitroxides are used, the thermal stability of these radicals and of the corresponding alkoxyamines represented a crucial point and has to be determined.[17,18]

In a previous study on the radical trapping properties of 3-aryl-2*H*-benzo[1,4]oxazin-4-oxides,[19] we noted the stability of the nitroxide spin adducts formed by the trapping of carbon-centered radicals, and as a consequence, we decided to prepare a series of new benzoxazine nitroxide radicals and to study their thermal stability.

RESULTS AND DISCUSSION

3-Substituted-3-aryl-2*H*-benzo[1,4]oxazin-4-oxyl radicals were prepared as summarized in Scheme 1, following a previously described procedure:[20] the appropriate Grignard reagent was added to the nitrone and the resulting hydroxylamine was then oxidized with lead dioxide.

The recorded EPR spectra of these nitroxides were interpreted on the basis of hfcc typical for this kind of radicals, in which the nitrogen three lines are mainly split by two different couples of aromatic hydrogens of the benzoxazine moiety: H(4) and H(11) with the larger hfcc (ca. 3 G) and H(7) and H(8) with the smaller one (ca. 1 G). In addition, the splitting of the two nonequivalent protons H(16) and H(17) are clearly visible, and in some derivatives such as **1b**, **1c**, and **1d**, further couplings with the R-group hydrogens are present. These assignments, confirmed by means of appropriate DFT calculations,[10] are reported in Table 1 together with the EPR parameters of all synthesized nitroxides.

The EPR spectra of all synthesized aminoxyls, together with their corresponding simulations, are collected in the Supporting Information, and as an example, the EPR signal of **1b** and its

Received: July 13, 2011
Published: October 17, 2011

Scheme 1. Synthesis of Derivatives 1−3(a−e) Showing the Arbitrary Atom Numbering

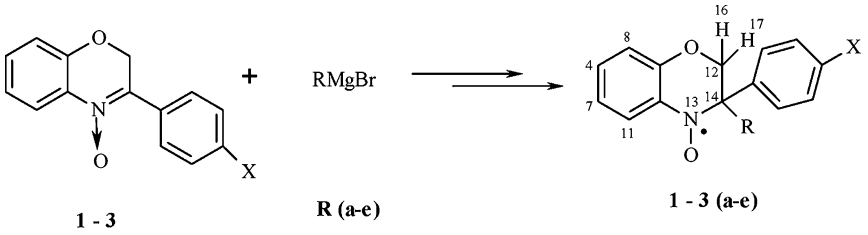

1 X = H
2 X = *p*-Cl
3 X = *p*-OCH_3

a R = C_6H_5
b R = $CH_2C_6H_5$

c R = CH_3
d R = CH_2CH_3
e R = $C(CH_3)_3$

Table 1. Hyperfine Coupling Constants and *g*-Factors of Nitroxides 1−3(a−e)[a]

	hfcc								
N−O•	H-4	H-7	H-8	H-11	H-16	H-17	N-13	H (R)	*g*
1a	−2.92	0.82	0.78	−2.81	0.38	0.73	10.67		2.0056_6
	(−2.91)	(1.02)	(1.01)	(−2.85)	(0.02)	(0.77)	(11.08)		
1b	−2.98	0.90	0.78	−2.86	0.27	0.75	10.84	0.48 (0.27)	2.0055_8
	(−2.99)	(1.09)	(1.05)	(−2.93)	(0.59)	(1.01)	(11.21)	0.39 (0.09)	
1c	−2.99	0.87	0.72	−2.90	0.32	0.71	10.64	0.50 (3H)	2.0055_8
	(−3.03)	(1.07)	(1.10)	(−2.95)	(0.65)	(1.01)	(11.07)	(0.34)	
1d	−2.99	0.87	0.79	−2.86	0.32	0.720	10.73	0.55 (0.29)	2.0056_5
	(−2.98)	(1.11)	(1.06)	(−2.95)	(0.57)	(0.98)	(11.17)	0.15 (0.06)	
1e	−2.81	0.77	0.77	−2.81	0.45	0.75	11.02	0.12 (9H)	2.0055_6
	(−2.90)	(1.03)	(1.02)	(−2.84)	(0.32)	(0.75)	(11.73)	(0.08)	
2a	−2.94	0.86	0.76	−2.81	0.35	0.73	10.70		2.0057_0
	(−2.91)	(0.01)	(1.01)	(−2.83)	(−0.09)	(0.75)	(11.10)		
2b	−2.98	0.88	0.79	−2.85	0.27	0.79	10.86	0.46 (0.28)	2.0055_8
	(−3.00)	(1.09)	(1.06)	(−2.92)	(0.51)	(0.99)	(11.24)	0.39 (0.11)	
2c	−2.99	0.87	0.75	−2.87	0.16	0.57	10.67	0.46 (3H)	2.0056_6
	(−2.94)	(1.05)	(1.03)	(−2.86)	(0.11)	(0.60)	(10.60)	(0.93)	
2d	−2.96	0.92	0.83	−2.84	0.34	0.72	10.70	0.50 (0.28)	2.0056_4
	(−3.00)	(1.09)	(1.06)	(−2.93)	(0.48)	(0.97)	(11.20)	0.19 (0.09)	
3b	−2.98	0.85	0.75	−2.86	0.27	0.76	10.89	0.49 (0.31)	2.0055_8
	(−2.98)	(1.10)	(1.06)	(−2.94)	(0.56)	(0.99)	(11.28)	0.39 (0.12)	

[a]Hyperfine coupling constants (hfcc) in Gauss. Computed values in parentheses. All data from deaerated benzene solutions. Refer to Scheme 1 for atom numbering.

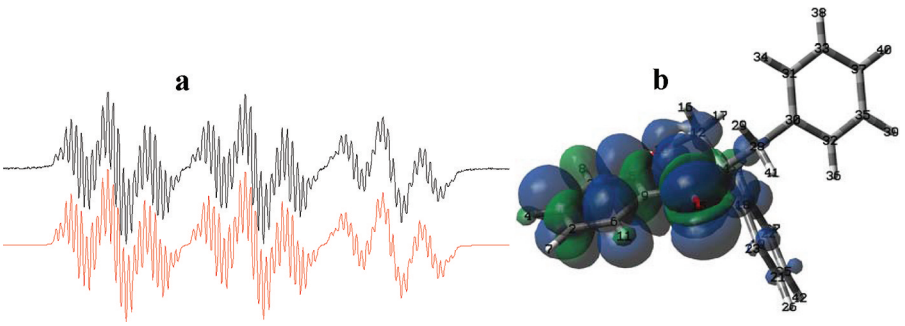

Figure 1. (a) Experimental (black) and simulated (red) EPR spectra of nitroxide **1b**; (b) spin density distribution ($\alpha-\beta$) of nitroxide **1b** computed at the B3LYP/EPR-III level (positive values in blue and negative in green).

spin density distribution plot are shown in Figure 1, where it can be observed the negative spin densities at H(4) and H(11) explaining the sign of their corresponding hfcc and why smaller hfcc values have been attributed to the other couple of aromatic protons H(7) and H(8).

As for indolinonic nitroxides,[10] this can be explained by considering the spin delocalization which occurs in these aminoxyls, as a consequence of the high level of coplanarity of the condensed rings of the benzoxazine moiety, shown by the molecular geometry of **1b** reported in Figure 2, and deduced by

dx.doi.org/10.1021/jo2014559 | *J. Org. Chem.* 2011, 76, 9253−9260

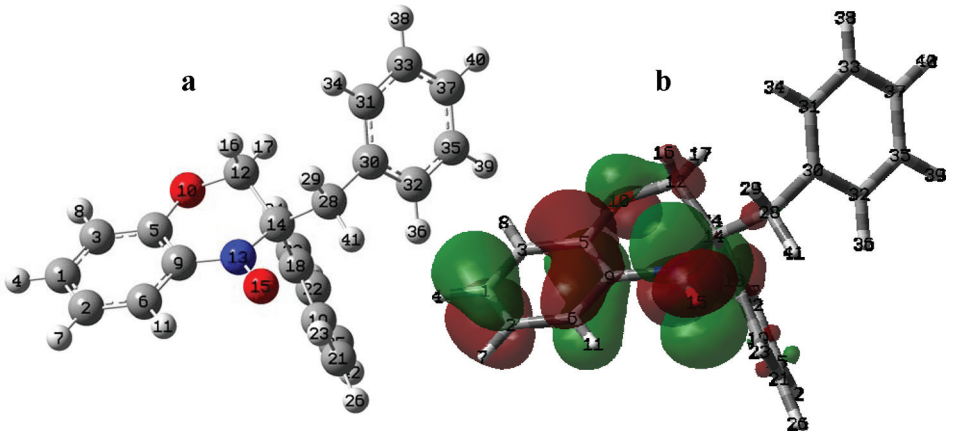

Figure 2. Ball and stick representation of the optimized geometry (a) and SOMO density plot (b) (positive values in red and negative in green) of nitroxide **1b** computed at the B3LYP/EPR-III level, showing the arbitrary atom numbering.

the geometric parameters computed at the PBE0/6-31G(d) level[21] reported in Table 2.

Table 2. Selected Bond Angles for of Nitroxides 1−3(a−e) Computed at the PBE0/6-31G(d) Level[a]

N−O•	O(15)−N(13)−C(9)−C(5)	O(10)−C(5)−C(3)−C(1)	O(15)−N(13)−C(9)−C(6)	C(14)−N(13)−C(9)	C(3)−C(5)−C(9)−C(12)
1a	172.24	179.80	5.41	118.95	12.78
1b	178.42	179.49	2.40	118.32	10.56
1c	177.88	179.52	2.77	118.33	10.46
1d	178.54	179.54	2.10	118.60	10.58
1e	177.37	179.67	1.18	118.71	11.20
2a	171.96	179.71	5.56	118.91	12.66
2b	179.02	179.63	1.94	118.35	10.62
2c	178.60	179.71	2.18	118.36	10.49
2d	179.43	179.75	1.47	118.60	10.61
3b	178.59	179.53	2.27	118.32	10.47

[a]Bond angles in degrees. Refer to Scheme 1 for atom numbering.

From the analysis of the data collected in Table 2, it can be observed that some dihedral angle values account for the coplanarity of the aminoxyl N−O group with respect to the aromatic ring, and that the C(14)−N(13)−C(9) angles values are very close to 120°, consistent with a N(13) strong sp^2 character; in addition, it can be estimated that C(12) lies outside of the benzoxazine imaginary plane defined by C(3)−C(5)−C(9) of about 10−12°.

All these geometrical features mainly refer to the benzoxazine moiety and do not depend on the particular R group present at C(14). For this reason, the same considerations may be applied to all nitroxides synthesized in the present work. Such a molecular structure allows the extension of the single occupied molecular orbital (SOMO), with its pronounced π character, over the whole benzoxazine system, as clearly shown by the distribution plot reported in Figure 2 for **1b**. Moreover, in both density plots reported in Figures 1 and 2, the different spin distribution on the diastereotopic protons H(16)/H(17) and H(29)/H(41) in **1b** is clearly visible, thus justifying the corresponding different hfcc values found.

Similarly to the experiments done in the past with indolinonic nitroxides,[17] the thermal stability of these new nitroxides was studied. It was carried out by means of EPR spectroscopy following the nitroxide signal decay with time at a specified temperature. In fact, according to the path described in Scheme 2, the nitroxide may undergo β-fragmentation on

Scheme 2. Thermal Fragmentation of Derivatives 1−3(a−e) to 1−3

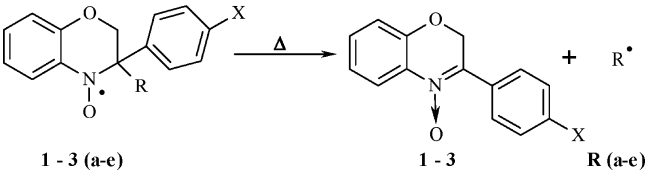

heating giving the diamagnetic nitrone **1−3** and the non persistent radicals **R(a−e)** (typical chromatograms are reported in the Supporting Information). Finally, these latter species could self-react or couple with a nitroxide molecule to form the corresponding alkoxyamine (N−OR in eq 2): both reactions are known to be very fast[7c−e] and to give EPR-silent species.[17]

Since the EPR signal recorded during the thermal fragmentation was due exclusively to the nitroxide under investigation, it was possible to use high modulation conditions so that the small signal splittings merged together and the complex EPR signal typical of these aminoxyls (see Figure 1a) was reduced to a broad triplet of triplets, which can be easily handled for kinetic measurements and, by repeating the experiments at different temperatures to determine the activation parameters.

A temperature range of 140−168 °C was used for such a study. In fact, since alkoxyamines are known to be thermally unstable and to give the parent radicals upon cleavage of the NO−C bond,[7a,b] in our experimental conditions the reversible reaction reported in eq 2 should be completely shifted to the left, so the measured decay constants should not be affected by this side reaction. In fact, as evidenced by the results of our experiments collected in Table 3, only aminoxyls **1b**, **1e**, **2b**, and **3b** showed detectable EPR signals decay at the different temperatures used (Figure 3), while no spectral variations were observed with time for derivatives **1−2a**, **1−2c**, and **1−2d**, even after 1 h of heating at the highest temperature employed in our tests. In other words, the only nitroxides undergoing thermal fragmentation are represented by derivatives with R = ^{t}Bu and R = CH_2Ph, hence releasing such "stabilized" C-centered radicals. As a consequence, the corresponding alkoxyamines eventually formed are known to be very unstable and should

dx.doi.org/10.1021/jo2014559 | J. Org. Chem. 2011, 76, 9253−9260

Table 3. Experimental Rate Constants (k), Half-Lives ($t_{1/2}$), and Activation Parameters for EPR Signal Decay in Deaerated *tert*-Butylbenzene Solutions of Derivatives 1b, 1e, 2b, and 3b

N−O•	T (°C)	$k \times 10^{3a}$	$t_{1/2} \times 10^{-3b}$	R^{2c}	$E_a{}^d$	log A ^{b}
1b	147.1	0.093	7.453	0.9779	37.34	16.21
	156.6	0.219	3.165			
	162.4	0.377	1.839			
	164.9	0.628	1.104			
1e	142.9	0.123	5.635	0.9908	34.46	14.21
	147.1	0.204	3.398			
	151.4	0.335	2.069			
	156.7	0.469	1.478			
	161.1	0.670	1.034			
	167.7	1.440	0.481			
2b	142.5	0.098	7.073	0.9360	35.88	15.58
	148.6	0.109	6.359			
	154.5	0.179	3.872			
	161.4	0.501	1.383			
	167.8	1.030	0.673			
3b	140.4	0.073	9.495	0.9984	36.39	15.80
	152.2	0.236	2.937			
	157.7	0.403	1.720			
	164.1	0.821	0.844			

^{a}In s^{-1}. ^{b}In s. ^{c}Correlation in the Arrhenius plot. ^{d}In kcal/mol.

decompose very quickly at the temperatures of our experiments to give the parent radicals (eq 2). In addition, a relatively high temperature range has been chosen to reduce experimental errors, since the same experiments carried out at temperatures lower than 140 °C yielded very uncertain decay traces, probably due to the relatively small fragmentation extent. On the other hand, at reaction temperatures higher than 180−200 °C it is known[17] that products arising from nitroxide and nitrone oxygen atom loss are formed. Moreover, in order to further reduce the possibility of experimental errors due to EPR line shape changes for the different temperatures employed, the peak-to-peak intensity variation with time was preferentially used instead of the corresponding peak areas.

Since the data reported in Table 3 show that only aminoxyls having a benzyl or a *tert*-butyl substituent at C(14) underwent thermal fragmentation, it can be summarized as follows:

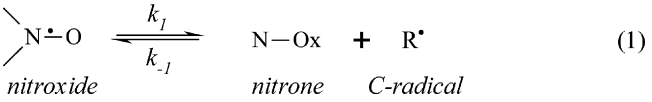

(1)

The C-centered radicals (R•) produced in this way may undergo very fast self-reactions but, at the same time, a fast reversible coupling with another aminoxyl molecule to yield the corresponding alkoxyamines (N−OR)[7c] is also possible:

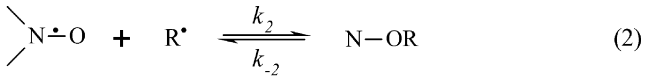

(2)

Both the above processes affect the EPR signal intensity whose decay can be written as:

$$-\frac{d[N-O^\bullet]}{dt} = k_1[N-O^\bullet] - k_{-1}[N-Ox][R^\bullet] + k_2[N-O^\bullet][R^\bullet] - k_{-2}[N-OR] \quad (3)$$

while for [R•]:

$$\frac{d[R^\bullet]}{dt} = k_1[N-O^\bullet] - k_{-1}[N-Ox][R^\bullet] - k_2[N-O^\bullet][R^\bullet] + k_{-2}[N-OR] \quad (4)$$

Considering that k_2 is usually very high ($k_2 \approx 10^9$ M^{-1} s^{-1}) while k_{-1}, referred to the addition of an alkyl radical to a nitrone, is usually about 4 orders of magnitude smaller, the term k_{-1}[N−Ox][R•] can be neglected and eqs 3 and 4 become

$$-\frac{d[N-O^\bullet]}{dt} = k_1[N-O^\bullet] + k_2[N-O^\bullet][R^\bullet] - k_{-2}[N-OR] \quad (5)$$

$$\frac{d[R^\bullet]}{dt} = k_1[N-O^\bullet] - k_2[N-O^\bullet][R^\bullet] + k_{-2}[N-OR] \quad (6)$$

Then, by applying the steady-state approximation, this last equation can be written as

$$k_1[N-O^\bullet] = k_2[N-O^\bullet][R^\bullet] - k_{-2}[N-OR] \quad (7)$$

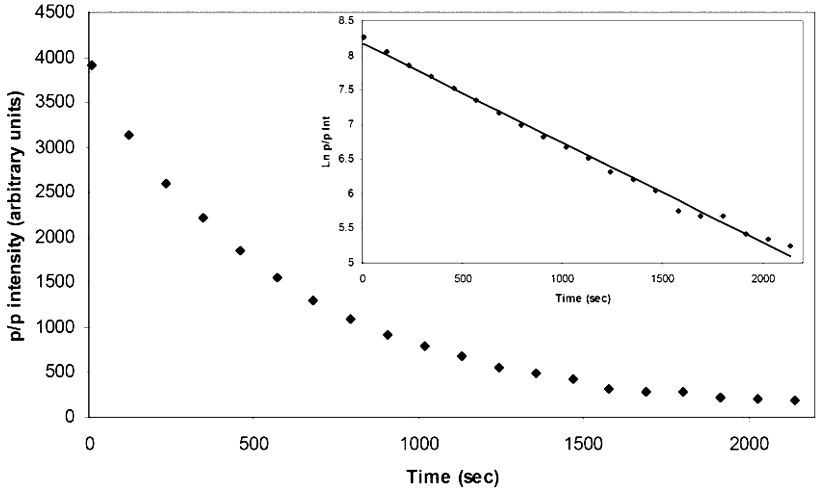

Figure 3. Signal decay trace (peak-to-peak intensity vs time) of nitroxide **1e** at 165 °C. In the inset the corresponding kinetic treatment is shown.

dx.doi.org/10.1021/jo2014559 | J. Org. Chem. 2011, 76, 9253−9260

and by substitution in eq 5 the aminoxyl consumption with time can be expressed as:

$$-\frac{d[N-O^{\bullet}]}{dt} = 2\bullet k_1[N-O^{\bullet}] \quad (8)$$

From these considerations, the EPR signal decay should follow first order kinetics, as observed experimentally, with a rate constant being twice the actual k_1.

As outlined previously, only aminoxyls with a benzyl or a *tert*-butyl group at C(14) underwent thermal fragmentation, i.e., when the leaving group is resonance stabilized or is a tertiary radical. From these findings, it could be supposed that the ease of aminoxyl fragmentation reflects the ease of formation of the corresponding leaving radical ($R^{\bullet}$), which in turn depends on its stability, thus affecting the C−C bond dissociation enthalpy (BDH). Such a thermodynamic quantity represents an important parameter for nitroxides modeling, since its DFT computation within a good degree of accuracy has recently become easier after the introduction of suitable functionals.[22]

In order to better understand the behavior of these nitroxides and to find possible correlations between their structure and their thermodynamic and kinetic properties, the C−C BDH and activation energies (E_a) of all aminoxyls synthesized in this work, independently from their thermal behavior, were computed using the M06-2X[23] and the MPW1K[24] functionals, respectively. The obtained values are reported in Table 4 together with the

Table 4. Experimental and Computed Activation Energies (E_a), Bond Dissociation Enthalpies (BDH), Computed C(14)−C(29) Bond Distances, And Imaginary Frequencies (i, in cm^{-1}) (BDH Values in Parentheses Have Been Computed According to Ref 25)

	E_a[a]					
N−O•	expt	calc[b]	BDH[a,c,d]	r[b,e]	r[b,e,f]	i[b,g]
1a		57.02	61.11	1.522	2.684	126.50
1b	37.34	37.12	40.11	1.545	2.451	304.87
1c		52.61	53.60	1.523	2.588	273.42
1d		48.95	51.92	1.534	2.588	252.09
1e	34.46	34.59	41.89 (36.09)	1.587	2.578	243.81
2a		56.88	61.14	1.522	2.686	123.31
2b	35.88	36.80	39.96	1.545	2.453	322.57
2c		52.84	53.26	1.523	2.587	270.94
2d		48.70	51.74	1.534	2.590	253.93
2e		34.53	41.70 (35.90)	1.586	2.580	243.00
3b	36.39	36.80	39.57	1.544	2.442	384.44

[a]In kcal/mol. [b]Computed at the MPW1K/6-31+G(d,p) level. [c]Computed at the M062X/6-31+G(d,p)//B3LYP/6-31G(d) level. [d]BDH values in parentheses have been computed according to ref 25. [e]r in Å. [f]Referred to the corresponding transition state. [g]Modes marked with negative sign in the corresponding frequency calculations.

C(14)−C(28) bond distances in the starting nitroxide and in the corresponding transition state (TS); for completeness, derivative **2e** is included in the table although not synthesized.

The data collected in Table 4 show that all computed E_a are in very good agreement with experimental ones, with the lowest values found for nitroxide **1e**, followed by the benzyl derivatives **1b**, **2b**, and **3b** (computational details in the Experimental Section). Since BDH should follow a similar trend, a correlation between these two quantities was checked, and it is plotted in Figure 4 (vide infra for the explanation of the "1−2e corr" term reported): a good correlation was found for all nitroxides

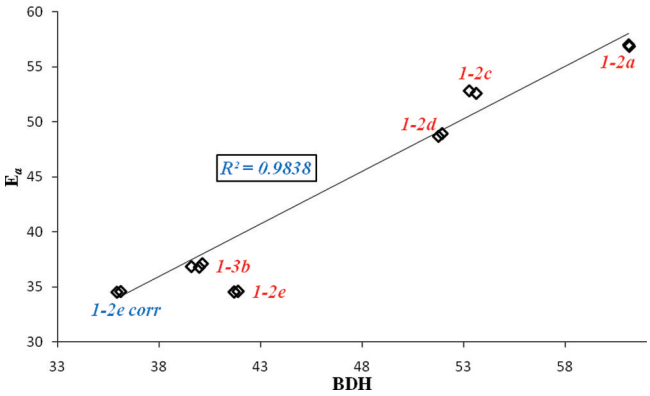

Figure 4. Plot of gas-phase E_a vs BDH for aminoxyls **1a−e**. Quantities in kcal/mol. See text for the "1−2e corr" value explanation.

except than **1e** and **2e** which lie outside the correlation line, suggesting that their BDH values result somewhat overestimated with respect to the corresponding (experimental) thermal fragmentation data.

However, as stated above, the fragmentation process should depend on the relative stability of the leaving radical $R^{\bullet}$ and hence on the BDH of the proper C−H bond in the corresponding hydrocarbon.[25,26] For this reason the BDE values of R−H were plotted vs the E_a and BDE of derivatives **1a−e** (Figure 5) and also in this case the data corresponding to **1e** lie out of the correlation.

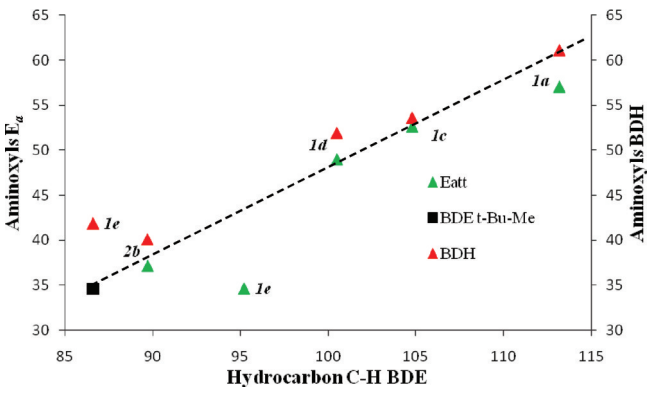

Figure 5. Plot of computed E_a (green) and BDH (red) of aminoxyls **1a−e** vs the of BDE of C−H (from ref 26) and C−C (in black, from ref 25) in the corresponding hydrocarbons. All quantities in kcal/mol.

In a previous paper on indolinonic nitroxides,[17] similar results were found and justified by considering a steric constraint eventually exerted by the bulky *tert*-butyl group.[27] The same explanation may apply also in the present case, especially if the relatively large C(14)−C(29) bond distances computed for **1e** and **2e** (Table 4) are considered (Figure 6). In fact, when BDH, which usually correlates with bond distances,[28] is plotted against the C(14)−C(29) bond length, a correlation was again found for all compounds rather than **1e** and **2e**.

The contribution of steric effects to the hydrocarbons R−H bond dissociation enthalpies, and the consequent choice of a reference compound different from the commonly used CH_3−H has recently been the subject of a considerable debate.[29,30] Zavitsas[25] considers the "strain free" BDH and the use of the C−C BDE in $(CH_3)_3C-CH_3$ instead of the corresponding C−H in $(CH_3)_3C-H$ seems to better reproduce the effect of steric

dx.doi.org/10.1021/jo2014559 | J. Org. Chem. 2011, 76, 9253−9260

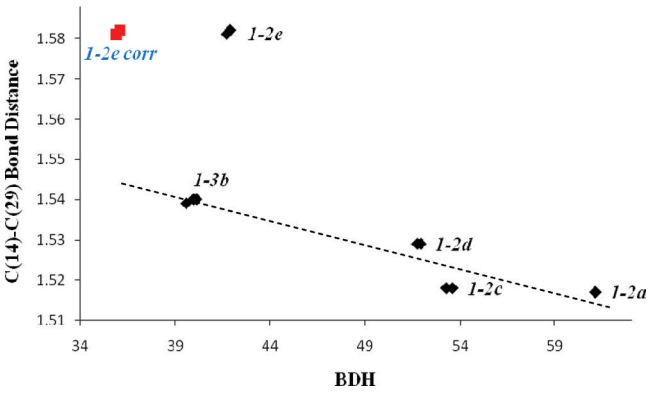

Figure 6. Plot of C(14)−C(29) bond distances (in Å) vs the corresponding BDH (in kcal/mol) of aminoxyls **1a−e**.

hindrance exerted by the *t*-Bu group. As a consequence, if the BDH value of $(CH_3)_3C-H$[26] is replaced with that of $(CH_3)_3C-CH_3$[25] in the plot of Figure 5, a better correlation is found, thus suggesting that in these fragmentations the steric contribution represents an important factor. Moreover, since the "steric strain" of the *tert*-butyl group has been estimated to be *ca* 5.8 kcal/mol,[25] by subtracting this quantity to the BDH values of **1e** and **2e**, (marked as "1−2e corr" values) a very good correlation (R^2 = 0.9819) was found also with E_a as shown in Figure 4. These results clearly indicate the important effect the steric hindrance of the substituent at C(14) has, together with the BDH values, on the thermal stability of these aminoxyls. Finally, a good correlation was found (R^2 = 0.9843) by replacing BDHs with the corresponding Gibbs free energy changes of the fragmentation reactions, as shown by the plot reported in Figure 7. This latter result could be explained by

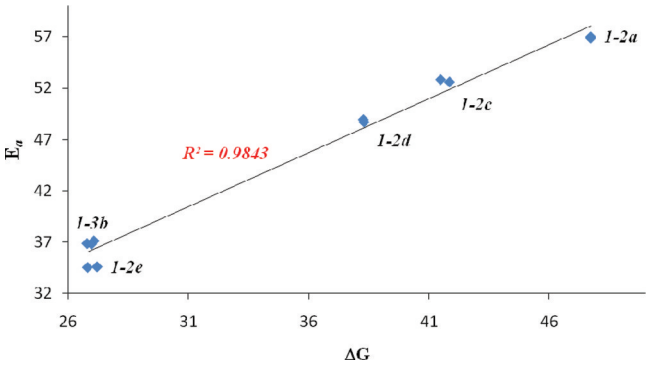

Figure 7. Plot of aminoxyls **1a−e** E_a vs the corresponding Gibbs free energy changes (Δ*G*). Quantities in kcal/mol.

assuming that the entropic component in Δ*G* should in some way include contributions from steric effects; as a consequence, it can be deduced that, from the thermodynamic point of view, a more "realistic" approach should consider reaction Free Energy rather than Enthalpy changes, especially for modeling purposes.

CONCLUSIONS

The newly synthesized 3-substituted-3-aryl-2*H*-benzo[1,4]-oxazin-4-oxyl nitroxides resulted stable in solutions at relatively high temperatures. Derivatives with a benzyl or a *tert*-butyl group in *β*-position to the aminoxyl function showed a thermal first order EPR signal decay likely due to the relative stability of the corresponding leaving radical. A deeper insight carried out by means of DFT calculations evidenced that in the case of the *tert*-butyl derivatives, steric hindrance should play a determinant role, not revealed by thermodynamics but by kinetics. For these reasons, it could be concluded that bond fragmentations could be heavily affected by the presence of "bulky" substituents, making the kinetic approach (i.e., E_a evaluations and/or computations) more "realistic", and hence preferable, in modeling studies with respect to the thermodynamic one based upon BDH comparisons. Finally, as far as thermodynamic is concerned, it appears that the best correlation with experimental E_a is found when the Gibbs free energy changes of the fragmentation reactions are considered instead of BDH values even in the presence of steric effects.

EXPERIMENTAL SECTION

General Methods. All chemicals were of the highest grade of purity commercially available and used without further purification. Melting points are uncorrected and were determined with an electrothermal apparatus. IR spectra were recorded in the solid state on a spectrophotometer equipped with a Spectra Tech collector for DRIFT measurements. Mass spectra were recorded in ESI mode with a TOF analyzer. Isotropic X-band EPR spectra were recorded on a spectrometer system equipped with a temperature controller, a microwave frequency counter, and an NMR gaussmeter for field calibration; for *g*-factor determination the whole system was standardized with a sample of perylene radical cation in concentrated sulfuric acid (*g* = 2.00258). General EPR spectrometer settings: microwave power 5 mW, modulation amplitude 0.1 G, field width 40 G, receiver gain 5 × 10^4. EPR spectral parameters for all the synthesized nitroxides are collected in Table 1.

General Procedure for the Synthesis of Benzoxazine Nitroxides. Nitrone **1−3**[19] (1 mmol) was dissolved in dry THF, and the proper Grignard reagent **Ra−e** (2 mmol) was added under a nitrogen stream. The reaction mixture was stirred at room temperature for 1 h; after this time, thin-layer chromatography (TLC) analyses showed the complete disappearance of the starting nitrone. The reaction was quenched with NH_4Cl and the mixture was extracted with Et_2O (3 × 10 mL). The ethereal solution was dried with Na_2SO_4 and filtered, lead dioxide was added to the solution, and the resulting mixture was stirred for 1 h. After this time, it was filtered and the solid was repeatedly washed with Et_2O. The solvent was evaporated under vacuum, and the residue was purified by SiO_2 column chromatography by eluting with cycloexane−ethyl acetate 9:1.

3,3-Diphenyl-2H-benzo[1,4]oxazin-4-oxyl (***1a***)*:* reddish oil; yield 82%; IR (neat, cm^{-1}) ν_{max} = 1588, 1482, 1389, 1226; HRMS calcd for $C_{20}H_{17}NO_2$ $[M + H]^+$ 303.1259, found 303.1258.

3-Benzyl-3-phenyl-2H-benzo[1,4]oxazin-4-oxyl (***1b***)*:* orange solid; mp 138−140 °C (absolute ethanol); yield 60%; IR (neat, cm^{-1}) ν_{max} = 1585, 1482, 1389, 1229; HRMS calcd for $C_{21}H_{19}NO_2$ $[M + H]^+$ 317.1416, found 317.1402.

3-Methyl-3-phenyl-2H-benzo[1,4]oxazin-4-oxyl (***1c***)*:* reddish oil; yield 46%; IR (neat, cm^{-1}) ν_{max} = 1587, 1484, 1392, 1231; HRMS calcd for $C_{15}H_{15}NO_2$ $[M + H]^+$ 241.1103, found 241.1110.

3-Ethyl-3-phenyl-2H-benzo[1,4]oxazin-4-oxyl (***1d***)*:* reddish oil; yield 80%; IR (neat, cm^{-1}) ν_{max} = 1586, 1483, 1392, 1229; HRMS calcd for $C_{16}H_{17}NO_2$ $[M + H]^+$ 255.1259, found 255.1250.

3-t-Butyl-3-phenyl-2H-benzo[1,4]oxazin-4-oxyl (***1e***)*:* reddish oil; yield 80%; IR (neat, cm^{-1}) ν_{max} = 1588, 1483, 1389, 1226; HRMS calcd for $C_{18}H_{21}NO_2$ $[M + H]^+$ 283.1572, found 283.1598.

3-p-Chlorophenyl-3-phenyl-2H-benzo[1,4]oxazin-4-oxyl (***2a***)*:* reddish solid; mp 118−120 °C (absolute ethanol); yield 85%; IR (neat, cm^{-1}) ν_{max} = 1587, 1483, 1383, 1224; HRMS calcd for $C_{20}H_{16}ClNO_2$ $[M + H]^+$ 337.0870, found 337.0897.

3-Benzyl-3-p-chlorophenyl-2H-benzo[1,4]oxazin-4-oxyl (***2b***)*:* reddish solid; mp 155−157 °C (absolute ethanol); yield 80%; IR (neat, cm^{-1}) ν_{max} = 1585, 1483, 1392, 1220; HRMS calcd for $C_{21}H_{18}ClNO_2$ $[M + H]^+$ 351.1026, found 351.1012.

dx.doi.org/10.1021/jo2014559 | *J. Org. Chem.* 2011, 76, 9253−9260

*3-Methyl-3-p-chlorophenyl-2H-benzo[1,4]oxazin-4-oxyl (**2c**):* reddish oil; yield 50%; IR (neat, cm^{-1}) ν_{max} = 1586, 1484, 1224, 1037; HRMS calcd for $C_{15}H_{14}ClNO_2$ $[M + H]^+$ 275.0713, found 275.0705.

*3-Ethyl-3-p-chlorophenyl-2H-benzo[1,4]oxazin-4-oxyl (**2d**):* red oil; yield 60%; IR (neat, cm^{-1}) ν_{max} = 1586, 1482, 1223; HRMS calcd for $C_{16}H_{16}ClNO_2$ $[M + H]^+$ 289.0870, found 289.0869.

*3-Benzyl-3-p-methoxyphenyl-2H-benzo[1,4]oxazin-4-oxyl (**3b**):* orange oil; yield 60%; IR (neat, cm^{-1}) ν_{max} = 1586, 1483, 1255, 1186, 1041; HRMS calcd for $C_{22}H_{21}NO_3$ $[M + H]^+$ 347.1521, found 347.1515.

General Procedure for the Thermal Decomposition of Benzoxazine Nitroxides. A *tert*-butylbenzene solution of the nitroxide (2×10^{-5} M) was thoroughly degassed with argon for 10 min and put into the EPR cavity at a given temperature, and the time-course of EPR spectra was monitored for 1 h, obtaining a set of 30 spectra. EPR spectrometer settings: microwave power 5 mW, modulation amplitude 1 G, field width 40 G, receiver gain 5×10^4. Rate constants were evaluated as averaged values from three to four independent runs at each temperature.

Computational Details. Density functional theory[12] calculations were carried out using the GAUSSIAN 09 suite of programs[31] on an IBM SP-6 at the Cineca Supercomputing Center.[32] All aminoxyl geometries were optimized at the B3-LYP/6-31G(d) level of theory and were carried out with the unrestricted formalism, giving $<S^2>$ = 0.7501 ± 0.0003 for spin contamination (after annihilation). Aminoxyls conformations were systematically screened by means of appropriate relaxed (i.e., with optimization at each point) potential energy surface scans to ensure that species were global minimum energy structures. In addition, in frequency calculations, imaginary (negative) values were never found, confirming that the computed geometries were always referred to a minimum. EPR parameters calculations were performed following the multistep procedure previously described.[10] Thermodynamic quantities were computed at 298 K by means of frequency calculations performed employing the M06-2X[23] functional in conjunction with the 6-31+G(d,p) basis set. Transition-state optimizations were performed employing the MPW1K functional[24] in conjunction with the 6-31+G(d,p) basis set for both optimizations and frequency calculations; in these last runs, all optimized stationary points were found to have the appropriate number of imaginary frequencies, and the imaginary modes (negative sign) corresponded to the correct reaction coordinates, also confirmed by their visualization with appropriate programs (animations files available as Supporting Information).

■ ASSOCIATED CONTENT

Supporting Information

Experimental and simulated EPR spectra and optimized geometries in Cartesian coordinates of all aminoxyls; Arrhenius plots for thermal fragmentations of derivatives **1**−**3b** and **1e**; optimized geometries of all fragmentation reactions Transition structures in Cartesian coordinates and animations of the corresponding imaginary frequencies as separate (.zip) files. This material is available free of charge via the Internet at http://pubs.acs.org/.

■ AUTHOR INFORMATION

Corresponding Author

*Fax: +39 071 2204714; Tel: +39 071 2204409 E-mail: p.stipa@univpm.it.

■ ACKNOWLEDGMENTS

MIUR (Ministero dell'Università e della Ricerca Scientifica e Tecnologica) is kindly acknowledged for financial support (PRIN 2008) and Cineca Supercomputing Center for computational resource allocation (ISCRA grant NMPALKOX, code: HP10CLBN2R).

■ REFERENCES

(1) (a) Mottley, C.; Mason, R. P. In *Biological Magnetic Resonance 8*; Berliner, L. J., Reuben, J., Eds.; Plenum Publishers: New York, 1989; p 489. (b) Engström, M.; Vaara, J.; Schimmelpfennig, B.; Ågren, H. *J. Phys. Chem. B* **2002**, *106* (47), 12354. (c) Ranby, B.; Rabek, J. F. In *ESR Spectroscopy in Polymer Research*; Springer Verlag: Berlin, 1971.

(2) (a) Berliner, L. J., Ed. *Molecular Biology Series: Spin Labeling, Theory and Applications*; Academic Press: New York, 1979; Vol. 2. (b) Haering, G.; Luisi, P. L.; Hauser, H. *J. Phys. Chem.* **1988**, *92*, 3574. (c) Subezynski, W. K.; Antholine, W. E.; Hyde, J. S.; Kusumi, A. *Biochemistry* **1990**, *29*, 736. (d) Marsh, D.; Watts, A.; Knowles, P. F. *Biochemistry* **1976**, *15*, 3570. (e) Berliner, L. J., Ed. *Biological Magnetic Resonance, Spin Labeling the Next Millenium*; Plenum Press: New York, 1998; Vol. *14*. (f) Strube, T.; Schiemann, O.; MacMillan, F.; Prisner, T. F.; Engels, J. W. *Nucleoside Nucleotide Nucl. Acids* **2001**, *20*, 1271. (g) Edwards, T. E.; Okonogi, T. M.; Robinson, B. H.; Sigurdsson, S. T. *J. Am. Chem. Soc.* **2001**, *123*, 1527. (h) Verma, S.; Eckstein, F. *Annu. Rev. Biochem.* **1998**, *67*, 99.

(3) Brash, R. C.; London, D. A.; Wesbey, G. E.; Tozer, T. N.; Nirecki, D. E.; Williams, R. D.; Doemeny, J.; Tuck, L. D.; Lallemand, D. P. *Radiology* **1983**, *147*, 773.

(4) Caneschi, A.; Gatteschi, D.; Rey, P. *Prog. Inorg. Chem.* **1991**, *39*, 331.

(5) (a) Klemchuk, P. P.; Gande, M. E. *Polym. Degrad. Stab.* **1988**, *22*, 241 and references cited therein. (b) Kocherginsky, N.; Swartz, H. M. In *Nitroxide Spin Labels, Reactions in Biology and Chemistry*; CRC Press: Boca Raton, 1995. (c) Stipa, P.; Astolfi, P.; Carloni, P.; Damiani, E.; Greci, L. In *Oxidants in Biology: A Question of Balance*; Valacchi, G., Davis, P., Eds.; Springer: Berlin, 2008; p 251.

(6) (a) Greci, L.; Damiani, E.; Carloni, P.; Stipa, P. In *Free Radicals in Biology and Environment*; Minisci, F., Ed.; Kluwer Academic Publishers: The Netherlands, 1997; p 223. (b) Samuni, A.; Krishna, M. C. In *Handbook of Synthetic Antioxidants*; Packer, L., Cadenas, E., Eds.; Marcel Dekker Inc.: New York, 1997; p 351. (c) Krishna, M. C.; Samuni, A. *Methods Enzymol.* **1994**, *234*, 580.

(7) (a) Howard, J. A.; Tait, J. C. *J. Org. Chem.* **1978**, *43*, 4279. (b) Grattan, D. W.; Carlsson, D. J.; Howard, J. A.; Wiles, D. M. *Can. J. Chem.* **1979**, *57*, 2834. (c) Chateauneuf, J.; Lusztyk, J.; Ingold, K. U. *J. Org. Chem.* **1988**, *53*, 1629. (d) Beckwith, A. L. J.; Bowry, V. W. *J. Org. Chem.* **1988**, *53*, 1632. (e) Khote, T.; Marque, S.; Martschke, R.; Popov, M.; Fisher, H. *J. Chem. Soc., Perkin Trans. 2* **1998**, 1553. (f) Stipa, P.; Greci, L.; Carloni, P.; Damiani, E. *Polym. Degrad. Stab.* **1997**, *55*, 323.

(8) (a) Barton, D. H. R.; Le Gloahec, V. N.; Smith, J. *Tetrahedron* **1998**, *39*, 7483. (b) Stipa, P. *J. Chem. Soc., Perkin Trans. 2* **2001**, 1793.

(9) (a) Howard, J. A. *Adv. Free Radical Chem.* **1971**, *4*, 161. (b) Khloplyankina, M. A.; Buchachenko, A. L.; Neiman, M. B.; Vasileva, A. G. *Kinetika Kataliz.* **1965**, *6*, 465. (c) Brownlie, I. T.; Ingold, K. U. *Can. J. Chem.* **1967**, *45*, 2427. (d) Pedersen, J. A; Torssel, K. *Acta Chem. Scand.* **1971**, *25*, 3151.

(10) Stipa, P. *Chem. Phys.* **2006**, *323*, 501.

(11) (a) Berti, C.; Colonna, M.; Greci, L.; Marchetti, L. *Tetrahedron* **1977**, *33*, 2321. (b) Berti, C.; Colonna, M.; Greci, L.; Marchetti, L. *Tetrahedron* **1977**, *33*, 3149. (c) Greci, L. *Tetrahedron* **1982**, *38*, 2435. (d) Cardellini, L.; Carloni, P.; Greci, L.; Stipa, P.; Faucitano, A. *Gazz. Chim. Ital.* **1989**, *119*, 621. (e) Damiani, E.; Carloni, P.; Stipa, P.; Greci, L. *Free Rad. Res.* **1999**, *31*, 113. (f) Carloni, P.; Damiani, E.; Scattolini, M.; Stipa, P.; Greci, L. *J. Chem. Soc., Perkin Trans. 2* **2000**, 447.

(12) (a) Parr, R. G.; Yang, W. In *Density Functional Theory of Atoms and Molecules*; Oxford University Press: New York, 1998. (b) Koch, W.; Holthausen, M. C. In *A Chemists Guide to Density Functional Theory*; Wiley-VCH: Weinheim, 2000.

(13) (a) Cimino, P.; Pedone, A.; Stendardo, E.; Menziani, M. C.; Crescenzi, O.; Barone, V. *Phys. Chem. Chem. Phys.* **2010**, *12*, 11697. (b) Improta, R.; Barone, V. *Chem. Rev.* **2004**, *104*, 1231. (c) Barone, V. In *Recent Advances in Density Functional Methods*; Chong, D. P., Ed.; World Scientific: Singapore, 1995; p 287. (d) Adamo, C.; Barone, V.; Fortunelli, A. *J. Chem. Phys.* **1995**, *102*, 384. (e) Adamo, C.; Barone, V.

J. Chem. Phys. **1999**, *110*, 6158. (f) Adamo, C.; Barone, V. *J. Chem. Phys.* **2002**, *116*, 593. (g) Malkin, V. G.; Malkina, O. L.; Eriksson, L. A.; Salahub, D. R. In *Modern Density Functional Theory, A Tool for Chemistry*; Seminario, J. M., Politzer, P., Eds.; Elsevier: New York, 1995. (h) Engels, B.; Eriksson, L. A.; Lunell, S. *Adv. Quantum Chem.* **1997**, *27*, 297. Batra, R.; Giese, B.; Spichty, M.; Gescheidt, G.; Houk, K. N. *J. Phys. Chem.* **1996**, *100*, 18371. (i) Chipman, D. M. *Theor. Chim. Acta* **1989**, *76*, 73. (j) Improta, R.; Scalmani, G.; Barone, V. *Chem. Phys. Lett.* **2001**, *336*, 349. (k) Ban, F.; Gauld, J. W.; Wetmore, S. D.; Boyd, R. J. In *EPR of Free Radicals in Solids: Trends in Methods and Applications*; Lund, A., Ed.; Kluwer Academic: Dordrecht, 2003; p 239. (l) Barone, V.; Cimino, P.; Pedone, A. *Magn. Reson. Chem.* **2010**, *48* (S1), S11−S22. (m) Cimino, P.; Pedone, A.; Stendardo, E.; Barone, V. *Phys. Chem. Chem. Phys.* **2010**, *12*, 3741.

(14) (a) Stipa, P.; Greci, L.; Alberti, A.; Sgarabotto, P.; Ugozzoli, F. *Tetrahedron* **1987**, *43* (13), 3031. (b) Damiani, E.; Carloni, P.; Stipa, P.; Greci, L. *Free Rad. Res.* **1999**, *31* (2), 113. (c) Dinoi, A.; Curci, R.; Carloni, P.; Damiani, E.; Stipa, P.; Greci, L. *Eur. J. Org. Chem.* **1998**, *5*, 871. (d) Carloni, P.; Greci, L.; Stipa, P.; Eberson, L. *J. Org. Chem.* **1991**, *56* (15), 4733. (e) Alberti, A.; Andruzzi, R.; Greci, L.; Stipa, P.; Marrosu, G.; Trazza, A.; Poloni, M. *Tetrahedron* **1988**, *44* (5), 1503. (f) Doepp, D.; Greci, L.; Nour-el-Din, A. M. *Chem. Ber.* **1983**, *116* (6), 2049.

(15) (a) Stipa, P.; Minaux, E.; Greci, L.; Bubak, M.; Tordo, P.; Senninger, T.; Carloni, P.; Damiani, E.; Tommasi, G. Eur. Pat. 014001937-2109, 2001. (b) Stipa, P.; Minaux, E.; Greci, L.; Bubak, M.; Tordo, P.; Senninger, T.; Carloni, P.; Damiani, E.; Tommasi, G., US Patent 6.531,556, 2003. (c) Stipa, P.; Minaux, E.; Greci, L.; Bubak, M.; Tordo, P.; Senninger, T.; Carloni, P.; Damiani, E.; Tommasi, G., US Patent 6.706.832, 2004.

(16) Guillaneuf, Y.; Gigmes, D.; Marque, S. R. A.; Astolfi, P.; Greci, L.; Tordo, P.; Bertin, D. *Macromolecules* **2007**, *40*, 3108.

(17) Stipa, P.; Greci, L.; Alberti, A.; Carloni, P.; Neri, C. *Polym. Degrad. Stab.* **1993**, *39*, 215.

(18) Stipa, P.; Greci, L.; Carloni, P.; Damiani, E. *Polym. Degrad. Stab.* **1997**, *55*, 323.

(19) Stipa, P.; Astolfi, P.; Marini, M. *J. Org. Chem.* **2007**, *72*, 8677.

(20) Berti, C.; Colonna, M.; Greci, L.; Marchetti, L. *Tetrahedron* **1975**, *31*, 1745.

(21) Adamo, C.; Barone, V. *J. Chem. Phys.* **1999**, *110*, 6158.

(22) (a) Zhao, Y.; Truhlar, D. G. *J. Chem. Phys.* **2006**, *125*, 194101. (b) Zhao, Y.; Truhlar, D. G. *Acc. Chem. Res.* **2008**, *41* (2), 157. (c) Zhao, Y.; Truhlar, D. G. *J. Chem. Theory Comput.* **2011**, *7*, 669.

(23) Zhao, Y.; Truhlar, D. G. *Theor. Chem. Acc.* **2008**, *120*, 215.

(24) Lynch, B. J.; Fast, P. L.; Harris, M.; Truhlar, D. G. *J. Phys. Chem. A* **2000**, *104*, 481.

(25) Matsunaga, N.; Rogers, D. W.; Zavitsas, A. A. *J. Org. Chem.* **2003**, *68*, 3158.

(26) Afeefy, H. Y.; Liebman, J. F.; Stein, S. E. Neutral Thermochemical Data. In *NIST Chemistry WebBook*; NIST Standard Reference Database No. 69 (http://webbook.nist.gov); Mallard, W. G., Linstrom, P. J., Eds.; National Institute of Standards and Technology: Gaithersburg, MD, 2005.

(27) It has to be noted that the *tert*-butyl radical rapidly decompose to isobutylene. Such a reaction is certainly responsible for the consumption of a certain amount of *tert*-butyl radicals from the reaction medium, but since its rate constant is close to k_2 and not far from the self-reaction rate constant between *tert*-butyls, we do not believe that such a behavior could significantly affect our kinetic measurements. In the present work this consideration is somehow supported by the good correlations, shown in Figures 4 and 5, found when appropriate corrections for the *tert*-butyl group steric strain are considered.

(28) Zavitsas, A. A. *J Phys. Chem A* **2003**, *107*, 897.

(29) Coote, M. L.; Lin, C. Y.; Beckwith, A. L. J.; Zavitsas, A. A. *Phys. Chem. Chem. Phys.* **2010**, *12*, 9597 and references cited therein.

(30) (a) Poutsma, M. L. *J. Org. Chem.* **2008**, *73*, 8921. (b) Wodrich, M. D.; McKee, W. C.; Schleyer, P. v. R. *J. Org. Chem.* **2011**, *76* (8), 2439.

(31) Gaussian 09, Revision B.01: Frisch, M. J.; Trucks, G. W.; Schlegel, H. B.; Scuseria, G. E.; Robb, M. A.; Cheeseman, J. R.; Scalmani, G.; Barone, V.; Mennucci, B.; Petersson, G. A.; Nakatsuji, H.; Caricato, M.; Li, X.; Hratchian, H. P.; Izmaylov, A. F.; Bloino, J.; Zheng, G.; Sonnenberg, J. L.; Hada, M.; Ehara, M.; Toyota, K.; Fukuda, R.; Hasegawa, J.; Ishida, M.; Nakajima, T.; Honda, Y.; Kitao, O.; Nakai, H.; Vreven, T.; Montgomery, J. A., Jr.; Peralta, J. E.; Ogliaro, F.; Bearpark, M.; Heyd, J. J.; Brothers, E.; Kudin, K. N.; Staroverov, V. N.; Kobayashi, R.; Normand, J.; Raghavachari, K.; Rendell, A.; Burant, J. C.; Iyengar, S. S.; Tomasi, J.; Cossi, M.; Rega, N.; Millam, N. J.; Klene, M.; Knox, J. E.; Cross, J. B.; Bakken, V.; Adamo, C.; Jaramillo, J.; Gomperts, R.; Stratmann, R. E.; Yazyev, O.; Austin, A. J.; Cammi, R.; Pomelli, C.; Ochterski, J. W.; Martin, R. L.; Morokuma, K.; Zakrzewski, V. G.; Voth, G. A.; Salvador, P.; Dannenberg, J. J.; Dapprich, S.; Daniels, A. D.; Farkas, Ö.; Foresman, J. B.; Ortiz, J. V.; Cioslowski, J.; Fox, D. J. Gaussian, Inc., Wallingford CT, 2009.

(32) Cineca Supercomputing Center, via Magnanelli 6/3, I-40033 Casalecchio di Reno, Bologna, Italy; http://www.cineca.it/HPSystems.